Journal of Atmospheric and Terrestrial Physics, 1972, Vol. 34, pp. 1647–1658. Pergamon Press. Printed in Northern Ireland

O^+, H^+ and He^+ ion distributions in a new polar wind model

J. LEMAIRE
Institut d'Aéronomie Spatiale de Belgique, Avenue Circulaire 3, B 1180, Bruxelles, Belgium

(*Received* 25 *April* 1972)

Abstract—In this paper it is shown how the hydrodynamic solutions of the polar wind can be fitted to the kinetic solutions applicable to the upper ionospheric polar regions where the Coulomb collisions are negligible. The bulk velocity and density distribution of the O^+, H^+ and He^+ are determined for boundary conditions deduced from the OGO 2 observations by TAYLOR *et al.* (1968), and for unequal ion and electron temperatures. The results are compared to the observations of HOFFMAN (1971) (Explorer 31) near 3000 km altitude.

Résumé—Dans ce travail on montre comment on peut raccorder les solutions hydrodynamiques du Vent Polaire aux solutions cinétiques applicables aux régions supérieures de l'ionosphère polaire où les collisions Coulombiennes sont négligeables. Les distributions de vitesse moyenne et de densité des ions O^+, H^+ et He^+ sont données pour des conditions de densité à 950 km déduites des observations de TAYLOR *et al.* (1968) (OGO 2) et pour des températures ioniques et électroniques inégales. Les résultats sont comparés aux observations de HOFFMAN (1971) (Explorer 31) au voisinage de 3000 km d'altitude.

1. INTRODUCTION

IN A RECENT paper, DONAHUE (1971) has clearly described the differences between hydrodynamic and exospheric Polar Wind models. He pointed out that both approaches are not contradictory but must be considered as complementary. The hydrodynamic model calculation introduced by BANKS and HOLZER (1968, 1969) or more recently by MARUBASHI (1970) is appropriated for the collision-dominated region (ion-barosphere), while the kinetic approach outlined by DESSLER and CLOUTIER (1968) and developed by LEMAIRE and SCHERER (1970, 1971) can only be used in the collisionless region of the polar ionosphere (ion-exosphere).

These two broad regions are separated by a narrow transition layer (100–200 km thick) where the Knudsen Number (Kn = the ratio of the Coulomb mean free path and the electron density scale height) increases rapidly from values much smaller than one to values larger than one. Neither the hydrodynamic Navier–Stokes equations, or any other higher approximation of the general transport equations (HOLT and HASKELL, 1965; CHAPMAN and COWLING, 1970), nor the kinetic or completely collisionless theory can describe precisely the structure of this transition region. More suitable mathematical techniques must then be used, e.g. Monte-Carlo or Particle In Cell (PIC) methods. Until accurate observations of this transition layer are available, it is probably not yet necessary to go into these details; it may therefore be assumed that the barosphere and exosphere are separated by a surface called the Baropause. This is defined as the level where the velocity dependent deflection mean free path of the charged particles, l, becomes equal to the electron density scale height, H, i.e. where $Kn = 1$.

BANKS and HOLZER's (1968, 1969) polar wind model is represented by the critical solution of the hydrodynamic transport equations in their Euler approximation. This is the unique hydrodynamic solution which, if prolonged in the exospheric region, would give a sufficiently small (scalar) pressure at very large radial distances.

The solution passes through a singular point which is a mathematical singularity for the non-linear differential equations considered. This singular point is at the altitude where the bulk velocity of the lightest ions changes from a subsonic to a supersonic flow regime.

When O^+ is the dominant ionic constituent, it has been shown by BANKS and HOLZER (1969) that the value of Kn at the singular point is slightly larger than 1·18, if the electron and ion temperatures are equal. Consequently, the baropause (where $Kn = 1$) is located below the altitude of the singular point (where $Kn \geqslant 1{\cdot}18$). A similar result is obtained by MARUBASHI (1970) and is clearly shown in the Fig. 14 of his paper. Therefore the singular point of the hydrodynamic theory is located in the exospheric region, and a kinetic theory can be used to describe the transition from the subsonic to the supersonic flow regime. Instead of prolonging the hydrodynamic solution above the baropause into the collisionless region, where its validity is *a priori* not easy to prove, we show in this paper how it is possible to extend the model by a kinetic type of solution.

In LEMAIRE and SCHERER's (1970, 1971) kinetic models, only the collisionless part of the polar ionosphere has been considered. The baropause was fixed at an arbitrary height of 2000 km where they assumed reasonable values of the O^+ and H^+ ion densities and temperatures.

As more precise experimental ion concentrations of the topside polar ionosphere are now available, we will use them to calculate new models, and show how it is possible to fit the hydrodynamic models for the barosphere to the kinetic models of the exosphere.

A comparison of hydrodynamic and exospheric calculations has been presented by HOLZER *et al.* (1971). They have shown that the density and bulk velocity profiles obtained in both approaches are not much different if the same boundary conditions are chosen at an exospheric level where the Knudsen number is larger than 1, and where the flow velocity is already supersonic. This results from the fact that the collisionless transport equations (governing exospheric models) and the hydrodynamic equations have the same leading terms when the collisions are unimportant, and when the bulk velocity is significantly larger than the sonic velocity.

2. THE MODEL

From the OGO 2 mass spectrometer measurements (TAYLOR *et al.*, 1968), it can be deduced that $n_{O^+} = 7 \times 10^3\ \mathrm{cm}^{-3}$ and $n_{H^+} = 3{\cdot}2 \times 10^2\ \mathrm{cm}^{-3}$ are typical ion concentrations in the dusk region of the sunlit polar cap at an altitude of 950 km, and for a dip latitude of about 85°S. We have used these values and an electron density of $n_{e^-} = 7320\ \mathrm{cm}^{-3}$ as boundary conditions at the reference level of 950 km. Assuming a constant electron and ion temperature of 2500°K and a neutral atmospheric model of 1000°K (NICOLET and KOCKARTS, private communication), we integrated the hydrodynamic continuity and momentum equations described by BANKS and HOLZER (1968, 1969).

The H^+ ions are produced by the charge exchange reaction ($H + O^+ \rightarrow H^+ + O$), and they are supposed to diffuse through a medium constituted of H, O and He atoms, O^+ ions and electrons in near static diffusive equilibrium. If n_{H^+} and w_{H^+} are respectively the H^+ number density and bulk velocity, the continuity equation

and the Euler approximation of the momentum equation are respectively

$$n_{H^+}w_{H^+}A = n_{H^+}(h_0)w_{H^+}(h_0)\,A(h_0) + \int_{h_0}^{h}(q_{H^+} - l_{H^+})A\,\mathrm{d}h = Q_{H^+}(h), \tag{1}$$

$$\frac{1}{w_{H^+}}\frac{\mathrm{d}w_{H^+}}{\mathrm{d}h}\left(\frac{{w_{H^+}}^2}{c^2} - 1\right) = \frac{\mathrm{d}\ln A}{\mathrm{d}h} - \left[1 - \frac{T_{e^-} - m_{O^+}}{(T_{e^-} + T_{O^+})m_{H^+}}\right]\frac{g}{c^2}$$
$$- \frac{w_{H^+}}{c^2}(\nu_{H^+,O^+} + \nu_{H^+,H} + \nu_{H^+,He} + \nu_{H^+,O}) - \left(1 + \frac{{w_{H^+}}^2}{c^2}\right)\frac{\mathrm{d}\ln Q_{H^+}}{\mathrm{d}h}, \tag{2}$$

with

$$c^2 = \frac{kT_{H^+}}{m_{H^+}}, \tag{3}$$

m_j is the mass of the j-particles; k the Boltzmann's constant; A is the section of the flux tube: $A \propto r^{-3}$; r is the geocentric radial distance; and g is the gravitational acceleration at the altitude h. The term $T_{e^-}m_{O^+}g/(T_{e^-} + T_{O^+})m_{H^+}$ corresponds in (2) to the upward electrostatic acceleration if $n_{H^+} \ll n_{O^+}$. (This last inequality is well satisfied in the collision-dominated region of the polar ionosphere where the hydrodynamic approximation will be considered.) The electrostatic polarization field is set up in the plasma by gravitional charge separation and results from the long-range interactions (Coulomb collisions with impact parameters larger than the Debye length, λ_D) of the charged particles in the plasma.

The third term in the r.h.s. of equation (2) is the frictional deceleration due to collision of H^+ with the neutral atoms and O^+ ions (Coulomb interactions with impact parameters smaller than λ_D). The collision frequencies, ν_{H^+j}, the production rate, q_{H^+}, and the loss rate, l_{H^+}, are taken from BANKS and HOLZER (1969).

Equation (2) was integrated by the Runge–Kutta method for boundary values at the reference level of 950 km altitude.

The solid lines in Fig. 1 show a family of hydrodynamic solutions corresponding to different hydrogen ion bulk flow speeds, w_{H^+}, or upward diffusion fluxes, F_{H^+}, at the reference level. These H^+ diffusion fluxes range from $F_{H^+} = 6{\cdot}4 \times 10^6$ cm^{-2} sec^{-1} to $3{\cdot}2 \times 10^7$ cm^{-2} sec^{-1} at 950 km altitude for the curves shown in Fig. 1.

The total collision frequency, ν_{H^+}, and the mean free path of the H^+ ions have been calculated at each altitude. These quantities are defined by

$$\nu_{H^+} = \nu_{H^+,O^+} + \nu_{H^+,H^+} + \nu_{H^+,H} + \nu_{H^+,O} + \nu_{H^+,He} \tag{4}$$

and

$$l_{H^+} = \left({w_{H^+}}^2 + \frac{3kT_{H^+}}{m_{H^+}}\right)^{1/2}\nu_{H^+}, \tag{5}$$

where the partial collision frequencies, $\nu_{i,j}$, are quoted from BANKS and HOLZER (1969) and SPITZER (1956). The vertical bars in Fig. 1 show the baropause altitude, h_0, where l_{H^+} is equal to the electron density scale height,

$$H = \left(\frac{\mathrm{d}\ln n_e}{\mathrm{d}r}\right)^{-1} \simeq \frac{k(T_{O^+} + T_{e^-})}{m_{O^+}g}. \tag{6}$$

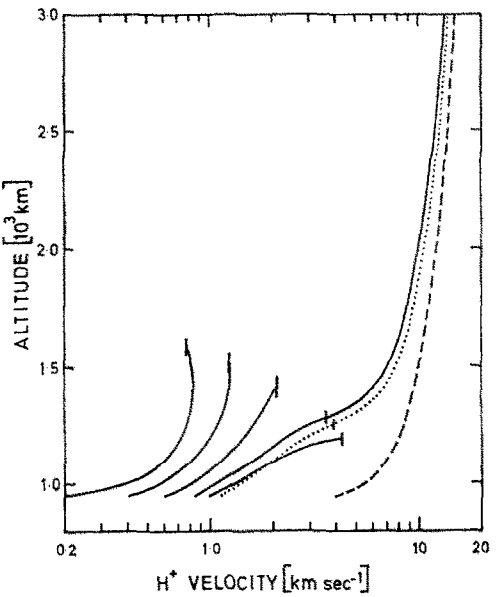

Fig. 1. Hydrogen ion bulk velocity versus altitude. The solid lines on the right hand side correspond to a family of hydrodynamic (type 1 and 2) solutions for five different values of the upward H^+ bulk velocity at the reference level of 950 km. The ion and electron temperatures are equal to 2500°K. The vertical lines on each of these curves show the baropause altitudes. Only one of these solutions fits the kinetic solution shown by the solid line on the left hand side. The dotted line corresponds to the solution when $T_{e^-} = T_{i^+} = 3000$°K. In all of these models the neutral particles are distributed according to the Nicolet and Kockarts model with a temperature of 1000°K. For comparison the dashed line gives w_{H^+} in a kinetic model whose baropause would be at 950 km and $T_{e^-} = T_{i^+} = 3000$°K.

Above this level the Coulomb collisions with impact parameters smaller than the Debye length, λ_D, become negligible. The global effect of the long-range particle interactions (Coulomb collisions with impact parameters larger than λ_D) can be described by a polarization electric field $\mathbf{E}$. For steady state conditions this electric field is derivable from a potential, Φ_E, whose altitude dependence is determined to maintain the local and global quasi-neutrality.

From Liouville's equation which reduces here to Vlasov's equation, it can be shown that the density of particles in phase space is constant along the particle trajectories

$$f(\mathbf{v}, h) = f(\mathbf{v}_0, h_0). \tag{7}$$

Therefore if $f(\mathbf{v}_0, h_0)$ is determined at the baropause, the velocity distribution and its moments (density, flux, pressure . . .) are determined at any altitude in the exosphere. The resulting density, flux, pressure tensors, etc. distributions are solutions of the collisionless transport equations.

Any parametric function of the velocity $\mathbf{v}_0$, whose ν first moments are equal to the ν corresponding moments of the actual velocity distribution can be chosen for $f(\mathbf{v}_0, h_0)$. In the following paragraph a one-parametric Maxwellian function is

chosen for each kind of particle j,

$$f_j(\mathbf{v}_0, h_0) = \begin{cases} 0; \text{ for } v_{0\parallel} < 0, \text{ and } v_0 > v_{j,\text{escape}} \\ N_j \left(\frac{m_j}{2\pi k T_j}\right)^{3/2} \exp\left[-\frac{m_j v_0^2}{2kT_j}\right]; \text{ otherwise.} \end{cases} \tag{8}$$

The subscripts $\parallel$ and $\perp$ denote the components parallel and perpendicular to the magnetic field; $v_{j,\text{escape}}$ is the velocity necessary for a particle j to escape along the open magnetic field lines. T_j is assumed to be equal to the j-ion temperature at the baropause. The parameters, N_j, are determined to match the density (the first moment of f) to its actual value just below the baropause: $n_j(h_0-)$,

$$n_j(h_{0+}) = \int f_j(\mathbf{v}_0, h_0)\, d\mathbf{v}_0 = n_j(h_0-). \tag{9}$$

As the H^+ ions are accelerated outwardly and do not have to overcome a barrier of potential to escape from the polar ionosphere, $v_{H^+,\text{escape}} = 0$ (LEMAIRE and SCHERER, 1970). Due to the truncation of the velocity distribution (8) to exclude incoming particles, it can be deduced from (8) and (9) that

$$n_{H^+}(h_{0+}) = \frac{N_{H^+}}{2} = n_{H^+}(h_0-), \tag{10}$$

and

$$F_{H^+}(h_{0+}) = \frac{N_{H^+}}{4}\sqrt{\frac{8kT_{H^+}}{\pi m_{H^+}}}. \tag{11}$$

From (10) and (11) it can be seen that the effusion velocity of the H^+ ions is given by

$$w_{H^+}(h_{0+}) = \sqrt{\frac{2kT_{H^+}}{\pi m_{H^+}}} = 0{\cdot}8\, c. \tag{12}$$

Among the family of hydrodynamic solutions described above and shown in Fig. 1, there is only one for which the bulk velocity, $w_{H^+}(h_0-)$, and the diffusion flux, $F_{H^+}(h_0-)$, at the corresponding baropause altitude, are precisely equal to the effusion velocity (12) and the escape flux (11). This hydrodynamic solution adopted here to describe the collision-dominated region is not necessarily the same as the critical solution selected by BANKS and HOLZER (1968, 1969) in their full hydrodynamic model calculation in order to pass through the singular point. However, at some reasonable distance below the baropause, both the critical solution and the solution for which the diffusion and escape fluxes are equal give nearly the same velocity profiles.

Above the baropause level, where the Knudsen number is larger than one, the kinetic theory of LEMAIRE and SCHERER (1970, 1971) is used to describe the distributions of the bulk velocity, the density, the parallel and perpendicular components of the kinetic pressure, etc.

3. Results and Discussions

The solid line at the right hand side of Fig. 1 shows the result of such a calculation for an electron and proton temperature of 2500°K. For higher values of

these temperatures, the H^+ bulk velocity and escape flux are enhanced as shown by the dotted line in Fig. 1, which corresponds to a model with an electron and ion temperature of 3000°K.

For comparison, the dashed line in Fig. 1 gives the H^+ velocity profile for a full kinetic model with the 'baropause' located a 950 km and a temperature of 3000°K for the charged particles.

The increase of the acceleration of the light ions in the transition region near the

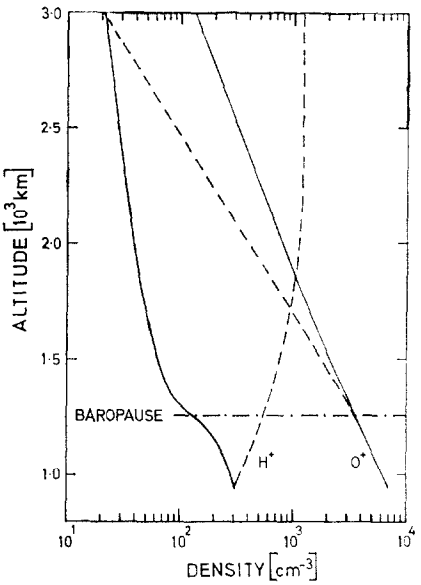

Fig. 2. Density distributions of oxygen, hydrogen and helium ions vs. altitude. The solid lines correspond to a polar wind model for which the electron and ion temperatures are equal to 3000°K (T_N = 1000°K). For comparison the dashed lines give the density distributions in the case of hydrostatic diffusive equilibrium.

baropause is a consequence of the electric force and of the rapid decrease of the frictional force with increasing streaming velocity when w_{H^+} approaches sonic values ($w_{H^+} \sim c$).

While in the full hydrodynamic polar wind models the transition from the subsonic to the supersonic regimes is a smooth and monotonic function of altitude (as in a Laval nozzle), in our models it has a steeper gradient in the altitude range where the collisions start to become less important.

The solid lines in Fig. 2 show the density distributions of O^+ and H^+ in a 3000°K polar wind model. The dashed lines correspond to a model where the ions would be in diffusive equilibrium above the reference level.

The slower decrease of the O^+ density in the dynamic case (solid line) is a consequence of the larger polarization electric field intensity, **E**, which maintains local and global quasi-neutrality, i.e. $n_{e^-}(h) = n_{O^+}(h) + n_{H^+}(h)$ and $F_{e^-} = F_{O^+} + F_{H^+}$. This can be seen in Fig. 3 where the ratio of the electric and gravitational forces acting upon an O^+ ion is given as a function of altitude for both of these models.

The dashed line gives the classical PANNEKOEK (1922)–ROSSELAND (1924) polarization field for a multicomponent ionosphere. At low altitudes, where O^+ dominates, the electric force is equal to one half of the gravitational force for the oxygen ions. At higher altitudes where H^+ would be the major constituant in a diffusive equilibrium mode, it is reduced by a factor of 16, so that $|eE/m_H g| = 0{\cdot}5$.

The solid line gives the value of $|eE/m_{O^+}g|$ for the dynamic model described in

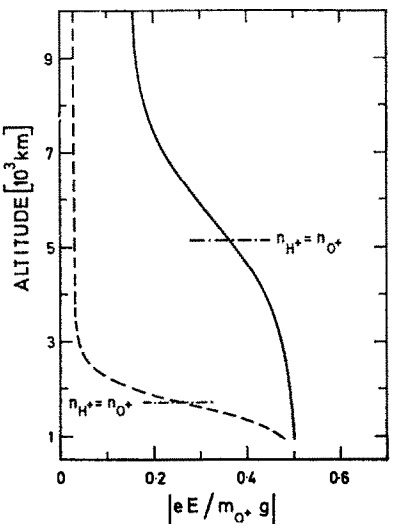

Fig. 3. Ratio of the electric and gravitational forces acting upon an O^+ ion vs. altitude. The solid line corresponds to a polar wind model for which the electron and ion temperatures are equal to 3000°K. The dashed line gives the corresponding ratio in the case of hydrostatic diffusive equilibrium for the same temperatures and reference level conditions. The altitude where the H^+ ions become more abundant than the O^+ ions are also shown for both the dynamic and static models.

Fig. 2. It can be seen that the electric field, which accelerates the H^+ ions, is much larger than in the static case. As a consequence, the electric potential, $\Phi_E(h)$, decreases faster along a given line of force in a dynamic model than in a static one: $[\Phi_E]_{h_0}^{h_1} = -1{\cdot}9$ V in the former case; $[\Phi_E]_{h_0}^{h_1} = -0{\cdot}7$ V in the latter one, for $h_0 = 1250$ km (baropause) and $h_1 = 10{,}000$ km.

It can also be seen from Figs. 2 and 3 that in dynamic models O^+ remains the predominant constituent up to higher altitudes.

It may be of interest to note that in the Polar Breeze model (DESSLER and CLOUTIER, 1968), the value of $|eE/m_{O^+}g|$ was assumed to be constant and equal to 0·5.

The last column in Table 1 summarizes some experimental results obtained by HOFFMAN (1971) when Explorer 31 was near 3000 km altitude in the sunlit polar cap region. Column A gives the ion densities and fluxes calculated in the previously discussed dynamic model corresponding to an electron and ion temperature of 3000°K. However, it is unlikely that the electrons and the different ions species are cooled at the same rate by collision with the low temperature neutral gas. Furthermore, heating by conduction and the transport of energy by convection will

Table 1. Comparison of ion densities and escape fluxes in two theoretical models with HOFFMAN's (1971) observations at 3000 km altitude

	A	B	HOFFMAN (1971)
T_{e^-}, $_{i^+}$[°K]	3000	4500 e^- 1500 O^+ 4000 H^+ 3750 He^+	
n_{O^+}[cm^{-3}]	150	130	80–100
n_{H^+}[cm^{-3}]	21	36	20–30
n_{He^+}[cm^{-3}]	–	0·87	–
F_{H^+}[cm^{-2} sec^{-1}]	3×10^7	$6{\cdot}7 \times 10^7$	5×10^7
F_{He^+}[cm^{-2} sec^{-1}]	–	$7{\cdot}1 \times 10^5$	5×10^5

affect in a different way the electrons, the heavy and the lighter ions. Reasonable values for the electron and ion temperatures seem to be: $T_{e^-} = 4500$°K, $T_{O^+} = 1500$°K, $T_{H^+} = 4000$°K, $T_{He^+} = 3750$°K. Indeed the electron and ion density scale heights in the polar topside ionosphere deduced from OGO 2 and OGO 4 ion measurements (TAYLOR *et al.*, 1968) or from Alouette I results (THOMAS and RYCROFT, 1970) can be interpreted with these unequal temperature values.

The results shown in the column B of Table 1 for an altitude of 3000 km are obtained for these temperatures by the method described in this paper and for $n_{O^+} = 7000$ cm^{-3}, $n_{H^+} = 320$ cm^{-3}, $n_{He^+} = 7$ cm^{-3} which are number densities measured by TAYLOR *et al.* (1968) at 950 km altitude in the polar ionosphere. The agreement with HOFFMAN's (1971) observations is quite satisfactory.

4. The Asymmetry of the Velocity Distribution

It has been argued that the velocity distribution function $f(\mathbf{v}_0, r_0)$ given by (8) is a questionable boundary condition for exospheric models because the H^+ ions have a large initial bulk velocity at the baropause (HOLZER *et al.*, 1971). It has also been suggested that a better approximation for $f_{H^+}(\mathbf{v}_0, h_0)$ would be

$$f_{H^+}(\mathbf{v}_0, h_0) = \begin{cases} 0; & \text{for } v_{0\parallel} < 0, \\ N_{H^+} \left(\dfrac{m_{H^+}}{2\pi k T_{H^+}}\right)^{3/2} \exp\left\{-\dfrac{m_{H^+}}{2kT_{H^+}}[(v_0 - u_{H^+})^2 + v_0^2]\right\}; & \text{otherwise,} \end{cases} \tag{13}$$

where N_{H^+} and u_{H^+} are the actual density $n_{H^+}(h_{0^-})$ and bulk velocity, $w_{H^+}(h_{0^-})$, just below the baropause.

In such an interpretation $f_{H^+}(\mathbf{v}_0, h_0)$ is chosen to approximate as closely as possible the actual velocity distribution for the outward flowing particles ($v_{0\parallel} > 0$). However, due to the truncation procedure (to exclude incoming particles: $v_{0\parallel} < 0$), the density and effusion velocity just above the baropause are not equal to $n_{H^+}(h_{0^-})$ and $w_{H^+}(h_{0^-})$ respectively. Therefore zero-order discontinuities in all the moments of the velocity distribution occur across the baropause boundary. MARUBASHI (1970) has tried to remove this inconsistency by calculating an appropriated value for u_{H^+} so that it is also equal to the 'effusion' velocity. The density discontinuity across the baropause has, however, not been removed in this attempt.

In our interpretation, $f(\mathbf{v}_0, h_0)$ is an appropriated boundary value for Vlasov's equation. It may be quite different from the actual velocity distribution, but its ν first moments coincide with those of the actual velocity distribution at the baropause and at any other altitude as a consequence of Liouville's theorem (7). For these moments which satisfy the collisionless transport equations, there will be no zero-order discontinuity across the baropause in the present interpretation. For instance, to match any number of moments of $f(\mathbf{v}_0, h_0)$ to their actual value at the boundary surface, a linear combination of truncated Maxwellian functions can be used for $f(\mathbf{v}_0, h_0)$,

$$\left(\frac{m}{2\pi k}\right)^{3/2} \sum_{s=1}^{\nu'} \frac{N^{(s)}}{T_\perp^{(s)}\, T_\parallel^{(s)1/2}} \exp\left[-\frac{m(v_{0\parallel} - u^{(s)})^2}{2kT_\parallel^{(s)}} - \frac{m{v_{0\perp}}^2}{2kT_\perp^{(s)}}\right], \tag{14}$$

where the parameters $N^{(s)}$, $u^{(s)}$, $T_\parallel^{(s)}$, $T_\perp^{(s)}$ can be determined by matching conditions at the baropause (e.g. equation (9)).

Although kinetic model calculations have been made by Scherer (private communication) for such a velocity distribution (14), it is, however, not necessary for the purpose of this paper to run into such a mathematical complication. As only the two first moments of the velocity distribution (density and bulk velocity) are available from experimental observations, (8) or (13) are sufficient approximations for the present aim.

If (13) is used instead of (8) in the kinetic model calculations, it can be shown that the effusion velocity is given by

$$w_{H^+}(h_{0^+}) = \sqrt{\frac{2kT_{H^+}}{\pi m_{H^+}}}\, \frac{e^{-U^2} + \sqrt{\pi}.U.Erfc(-U)}{Erfc(-U)}, \tag{15}$$

where

$$U^2 = \frac{m_{H^+}{u_{H^+}}^2}{2kT_{H^+}} \tag{16}$$

and

$$Erfc(-U) = \frac{2}{\sqrt{\pi}} \int_{-U}^{\infty} e^{-y^2}\, dy. \tag{17}$$

In the 'symmetric' case ($u_{H^+} = U = 0$), equation (12) is recovered, and $w_{H^+}(h_{0^+})$ is smaller than c, the critical velocity of the hydrodynamic theory. For $u_{H^+} = 0{\cdot}48\ c$, $w_{H^+}(h_{0^+}) = c$. When u_{H^+} is much larger than c, $w_{H^+}(h_{0^+}) \lesssim u_{H^+}$.

For $0{\cdot}48\ c < u_{H^+} < \infty$, as in Holzer's *et al.* (1971) semi-kinetic model, $c < w_{H^+}(h_{0^+}) < \infty$; and the hydrodynamic solution, which will fit this supersonic effusion velocity cannot be one of the fully subsonic solutions (type 1; e.g. in Fig. 1) with a bulk velocity never reaching supersonic values. Neither can it be a subsonic solution with a bulk velocity larger than that of the critical solution (type 2; e.g. in Fig. 1). [Note that this second type of solution has been found to fit the kinetic models when $u_{H^+} = 0$ or more generally when $0 < u_{H^+} < 0{\cdot}48\ c$.] The solutions of type 2 must, however, be excluded when $u_{H^+} > 0{\cdot}48\ c$ because they are not defined beyond the altitude where w_{H^+} becomes equal to c (see Banks and Holzer, 1969, for a description of the different branches of the hydrodynamic solutions). Moreover,

the critical solution separating the types 1 and 2 must also be excluded. Indeed, for this peculiar solution the baropause had to be located in the supersonic region, above the altitude of the singular point. But this contradicts the fact that the Knudsen number is already larger than 1 at the singular point ($Kn \geqslant 1{\cdot}18$ when $T_{e^-} = T_{i^+}$; see BANKS and HOLZER, 1969), and that the baropause (where $Kn = 1$) is consequently located in the subsonic region, i.e. below the altitude of the singular point. There remains another branch of hydrodynamic solutions (type 4) for which the bulk velocity is supersonic in the whole altitude range and for which w_{H^+} increases

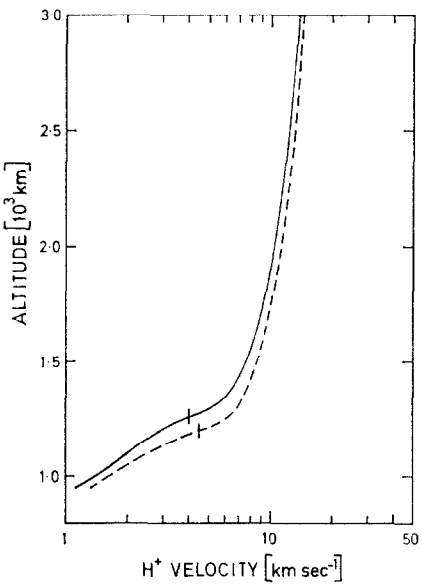

Fig. 4. Hydrogen ion bulk velocity vs. altitude. The solid line corresponds to a model with $u_{H^+} = 0$ (symmetric case). The dashed line corresponds to a model with $u_{H^+} = 0{\cdot}28\ c = 1{\cdot}41$ km sec^{-1} (asymmetric case). The vertical bars indicate the location of the baropause. In these models it is assumed that $T_{e^-} = T_{i^+} = 3000°$K and $T_N = 1000°$K.

rapidly with decreasing altitudes in the collision-dominated region. Although among this fourth type of hydrodynamic solutions there is one which will fit any kinetic model with $u_{H^+} > 0{\cdot}48\ c$, it is obvious that they are of no help in a description of the polar wind flow because of their behavior in the low altitude range.

Therefore, no hydrodynamic solution with a subsonic flow velocity in the low altitude (collision-dominated) region can be found to fit kinetic models with supersonic effusion velocities (i.e. $u_{H^+} > 0{\cdot}48\ c$). It can be concluded that only kinetic models with effusion velocities smaller than c (i.e. $u_{H^+} < 0{\cdot}48\ c$) are to be considered in exospheric theories of the polar wind.

It will now be shown that the effect of the asymmetry parameter, u_{H^+}, on the density and bulk velocity distribution is small unless unrealistic values of u_{H^+} are assumed in (13).

The dashed lines in Figs. 4 and 5 give the bulk velocity and density distribution

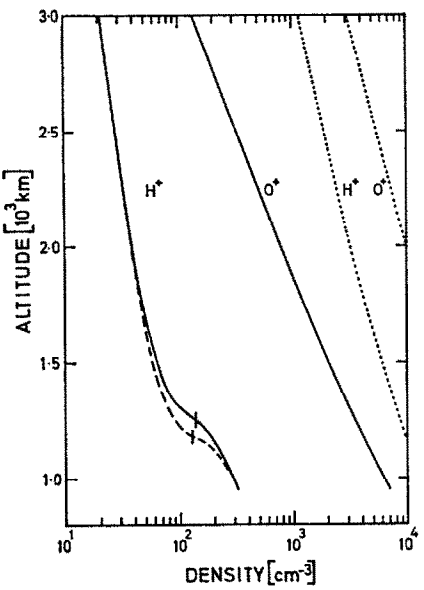

Fig. 5. Oxygen and hydrogen ion densities versus altitude. The solid lines correspond to a model with $u_{H^+} = 0$ (symmetric case). The dashed lines correspond to a model with $u_{H^+} = 0{\cdot}28\ c = 1{\cdot}41$ km sec^{-1} (asymmetric case). The dotted line show BANKS' and HOLZER's (1969) hydrodynamic model. In all these models it is assumed that $T_{e^-} = T_{i^+} = 3000$°K and $T_N = 1000$°K.

in an asymmetric case, i.e. for $u_{H^+} = 0{\cdot}28\ c = 1{\cdot}41$ km sec^{-1}. The solid lines show the corresponding distributions for the symmetric case, i.e. for $u_{H^+} = 0$. In both models $T_{e^-} = T_{i^+} = 3000$°K.

When u_{H^+}/c is increased from 0 to 0·28, (i) the effusion velocity is increased from 0·8 c to 0·91 c; (ii) the baropause density of H^+ is decreased by 7 per cent; (iii) the escape flux is increased by 3 per cent; and (iv) the baropause altitude is lowered by 65 km as a consequence of the larger mean velocity at the baropause. Indeed the mean free path of a charged particle increases with its velocity (see equation (5)) and the Knudsen number becomes equal to 1 at a lower level where n_{O^+} is larger.

This example shows that the degree of asymmetry of the velocity distribution $f(\mathbf{v}_0, h_0)$ at the baropause has not the considerable importance that has sometimes been inferred.

For comparison, the dotted lines in Fig. 5 give the density distributions of BANKS and HOLZER's (1969) hydrodynamic model with the same neutral and charged particles temperatures as in the model A. As the ion densities in this work are much larger than in our models, the singular point of their hydrodynamic model is located at a much higher altitude than the baropause in our models which are based on observed ion densities at a reference level of 950 km.

CONCLUSIONS

It has been shown in this paper that kinetic and hydrodynamic models can be fitted together at the baropause level which is the common frontier of the

collision-dominated plasma (governed by hydrodynamic transport equations) and the ion-exosphere (where the collisionless transport equations are suitable).

For observed ion densities at a reference level of 950 km and reasonable values for the temperatures, a hydrodynamic solution has been determined to fit the effusion velocity and the escape flux at the level where the collision mean free path becomes equal to the density scale height. The solution so obtained is not the usual critical solution but has a slightly larger bulk velocity in the subsonic (low altitude) region. The density and flux of H^+ and He^+ are in satisfactory agreement with the observations at 3000 km.

It has also been shown that the asymmetry of the velocity distribution cannot be too large unless a full supersonic hydrodynamic solution is to be used to describe the flow of H^+ in the collision-dominated (low altitude) region. In this paper the degree of asymmetry remains a free parameter in the velocity distribution (13). In more elaborated models this parameter can always be chosen to fit some supplementary boundary condition. However, the effect of such an asymmetry on the bulk velocity and density distributions has been shown to be relatively unimportant.

Acknowledgements—The author is grateful to Prof. M. NICOLET for his encouragements and to Dr. M. SCHERER for useful discussions. Helpful suggestions by a referee have been much appreciated.

REFERENCES

BANKS P. M. and HOLZER T. E. 1968 *J. geophys. Res.* **73,** 6846.

BANKS P. M. and HOLZER T. E. 1969 *J. geophys. Res.* **74,** 6304; 6317.

BANKS P. M. 1969 *The Polar Ionosphere and Magnetospheric Processes.* Scovli, Gordon and Breach, New York.

CHAPMAN S. and COWLING T. G. 1970 *The Mathematical Theory of Non-Uniform Gases* (3rd edn). Cambridge University Press.

DESSLER A. J. and CLOUTIER P. A. 1969 *J. geophys. Res.* **74,** 3730.

DONAHUE T. M. 1971 *Rev. Geophys. Space Phys.* **9,** 1.

HOFFMAN J. H. 1971 *Trans. Am. Geophys. Un.* **4,** 301.

HOLT E. H. and HASKELL R. E. 1965 *Foundations of Plasma Dynamics,* pp. 275–276. Macmillan, New York.

HOLZER T. E. 1969 *Polar Ionosphere and Magnetospheric Processes.* Scovli, Gordon and Breach, New York.

HOLZER T. E., FEDDER J. A. and BANKS P. M. 1971 *J. geophys. Res.* **76,** 2453.

LEMAIRE J. and SCHERER M. 1970 *Planet. Space Sci.* **18,** 103.

LEMAIRE J. and SCHERER M. 1971 *Phys. Fluids* **14,** 1683.

MARUBASHI K. 1970 *Rep. Ionos. Space Res. Japan* **24,** 322.

PANNEKOEK A. 1922 *Bull. Astron. Inst. Neth.* **19,** 107.

ROEDERER J. G. 1969 *Rev. Geophys.* **7,** 77.

ROSSELAND S. 1924 *Mon. Not. R. Astron. Soc.* **84,** 720.

TAYLOR H. A., JR., BRINTON H. C., PHARO M. W. III and RAHMAN N. K. 1968 *J. geophys. Res.* **73,** 5521.

THOMAS J. O. and RYCROFT M. J. 1970 *Planet. Space Sci.* **18,** 41.